Highlights

Femtosecond optical parametric oscillator with 3D-printed polymeric parts

Federico Pirzio, Jacopo Rubens Negri, Antonio Agnesi

- A synchronously-pumped fs OPO pumped at 800 nm and based on MgO:PPLN was developed.
- Low-cost 3D printing was exploited for the critical cavity pump/focusing section.
- A detailed characterization of the SPOPO with state-of-the-art performance is shown.
- Despite using 3D-printed plastic long-term stability in lab conditions was obtained.

Femtosecond optical parametric oscillator with 3D-printed polymeric parts

Federico Pirzio[a,1], Jacopo Rubens Negri[b], Antonio Agnesi[a]

[a] *Dipartimento di Ingegneria Industriale e dell'Informazione, Universita' di Pavia, Via Ferrata 5, Pavia, 27100, Italy*
[b] *Bright Solutions Srl, Via degli Artigiani 27, Cura Carpignano (PV), 27010, Italy*
[c] *Corresponding Author - email: federico.pirzio@unipv.it; Tel.: +39 0382985225; Fax: +39 0382422583,*

Abstract

A synchronously-pumped optical parametric oscillator (SPOPO) based on a periodically-poled, MgO-doped lithium niobate (MgO:PPLN) crystal was realized exploiting additive manufacturing technology for the pump and focusing section of the cavity, where careful predesign of the tightly-packed mounts and optics can be very helpful in view of a more traditional mechanical realization. Surprisingly, the 3D-printed plastic parts ensured long-term stability of the (quite sensitive, in principle) femtosecond SPOPO.

Keywords: Laser Materials, Solid-state Lasers, Ytterbium Doped Lasers

1. Introduction

Femtosecond single-resonant SPOPOs based on Ti:sapphire pump lasers is well-known technology, developed since early 1990s [1, 2]. Commercial development soon followed and there are now several companies offering such products.

Meanwhile, PPLN has been quickly establishing as a reliable commercial crystal with very high nonlinearity and figure of merit 90 times that of lithium triborate (LBO). In particular, the congruent growth process with MgO-doping to alleviate parasitic photorefraction, has provided outstanding results both for high-power applications and for convenient room-temperature operation [3]-[9].

Additionally, PPLN has a transparency range that extends into the mid-infrared, which is beneficial for generating idler wavelengths as long as 5 μm [9] for gas-sensing applications, for example.

A femtosecond SPOPO operating in the telecom wavelength range 1.3 - 1.6 μm was necessary for ongoing research work in our Department. The simplest and most affordable solution was the modification of a LBO SPOPO setup that was already available on a breadboard. Future projects will require also 2 - 4 μm wavelengths, hence MgO:PPLN was a natural choice for the nonlinear crystal.

Three-dimensional (3D) printing based on fused deposition modeling has been recently established as a cost-efficient and time-saving technology for fabricating a variety of different items. However, in the field of optics, it is nowadays mostly used for realization of THz components [10]. This can be explained by the combination of the favourable optical properties of polymers in the THz domain for the materials used in the fused deposition as well as a printing resolution, typically around 50-100 μm even for low-cost 3D-printers, which provides sub-wavelength accuracy to realize components with good performance [11].

In this work we explored the possibility to apply 3D printing to laser source design, in particular exploiting it as a cost-effective and time-efficient tool in the initial stage of the mechanical design of a laser prototype.

Although the thermo-mechanical properties of the thermoplastic polyester (PLA) frequently used for 3D printing are inferior to those of conventional machined metal plates, in particular the thermal expansion coefficient $\sim 8.5{\cdot}10^{-5}$ K^{-1} [12] ($\sim$ 4 times that of aluminum, $\sim$ 70 times that of Invar), we wanted to see whether this technology might be suitable at least in a preliminary stage of design, since in principle it is very handy and inexpensive for the few iterations required to optimize the opto-mechanical layout of this and many other laser systems. The femtosecond SPOPO seemed an excellent test opportunity in this regard, being a system quite sensitive to thermo-mechanical perturbations (cavity length changes and misalignments). Incidentally, we observed that the thermo-mechanical properties of the 3D printed parts were good enough to guarantee reliable and long-term stable operation even for this generally complex and environmental-sensitive laser source.

2. Experimental setup and results

A commercial mode-locked Ti:sapphire laser was already available as a pump laser at 80 MHz repetition rate, delivering $\sim$ 130-fs pulses at 790 - 820 nm where Kerr-lens mode-locking operation is more robust. For the SPOPO we kept the nearly-symmetric Z-shaped (folded) cavity design of Fig. 1,

requiring minor changes to the existing setup based on a non-critically phase-matched LBO, similar to that reported in Ref. [13].

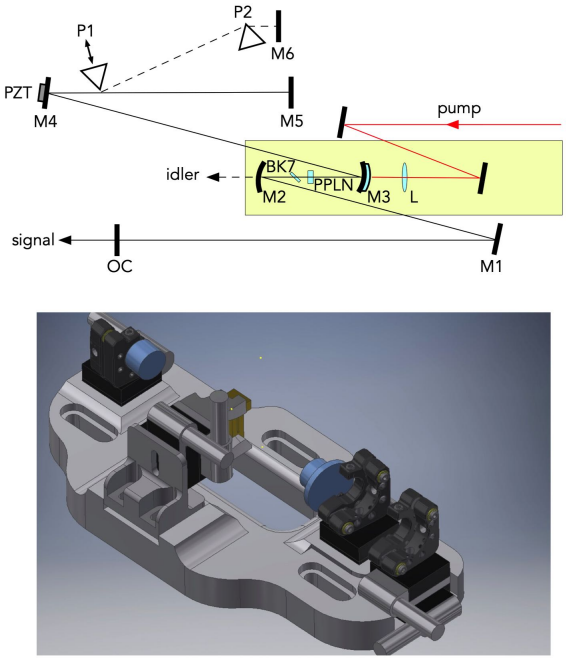

Figure 1: SPOPO layout. All mirrors M1-M6 are high-reflectivity at 1.3-1.6 μm. M3 is also high-transmittivity at 800 nm. SF10 prisms P1-P2 could be inserted in the cavity optionally. PZT is a piezo-transducer for wavelength stabilization. CAD picture: implementation with 3D-printed parts.

Besides tunability limitations, both high-temperature operation and exposition to ambient air contributed to damage events of the uncoated Brewster-cut faces of the LBO crystal over the years, requiring repolishing several times before this more radical upgrade was decided. A set of dielectric mirrors, high-reflectivity at 1.3 - 1.6 μm, with an output coupler (OC) of 7% transmittivity were also available. Signal wavelength stabilization for long-term operation was achieved through a servo-loop with the piezo-driven mirror M4 [13, 14].

The replacement, readily available commercial MgO:PPLN crystal was 1-mm thick, with input/output faces 1×14 mm^2, AR-coated at $\sim$ 800 nm and at $\sim$ 1.15 - 1.6 μm, with a fan-shaped grating (Λ = 20.5 - 23.5 μm along the 14-mm side).

From the mechanical point of view, the most critical part of the setup regards the pump and resonator focusing section, where mounts must be

packed in a tight space, with the thin (normal-incidence) nonlinear crystal and all the necessary translation stages, ensuring precise alignment of the pump and signal beam between the concave mirrors M2 and M3 (with 100-mm radius-of-curvature).

To this aim we 3D-printed a polymeric interface for a coarse pre-alignement of mount/optics in the yellow box in Fig. 1. Such plate could then be attached to the breadboard using the existing threaded holes. Micrometric translation stages and kinetic mirror mountings could be mounted on the polymeric plate with passing-through screws. The polymeric interfaces were manufactured by means of fused filament deposition modeling 3D printer (Sharebot NG, Sharebot S.r.l.). The minimal layer thickness achievable with this 3D printer is 50 μm, but in our case, we opted for a layer thickness of 100 μm to trade-off printing quality for speed. In this working conditions, the approximate printing time of the base plate shown in Fig. 1 is 10 hours. The infill pattern was hexagonal with a fill density of 30%. The interfaces were designed with CAD software, whereas the slicing software employed to generate the gcode was the open-source Slic3r [15].

Both concave mirrors M2, M3 were mounted on precision micrometric translation stages, as well as the MgO:PPLN holder that was also equipped for temperature control (which turned out to be non-essential, since the crystal could be conveniently operated at room temperature, according to the manufacturer). Pump was focused through an AR-coated lens L at normal incidence with 100-mm focal length, also on precision translation stage, producing a $\sim$ 50-μm pump spot diameter matching the cavity mode waist, while a second 200-mm focal length plane-concave AR-coated lens was put in contact with M3 to cancel its negative dioptric power.

We originally planned to commission the machining of the final metal interface to a workshop. However, this proved to be unnecessary: we configured the SPOPO cavity for operation in the stability region with lowest misalignment sensitivity, i.e. large separation between curved mirrors M2-M3, $\sim$ 106 mm (see Fig. 2). Over months of operation, we never observed performance degradation of the SPOPO using these 3D-printed interfaces, nor day-to-day operation stability was affected.

For comparison, we also tested the SPOPO working with shorter separation M2-M3 $\sim$ 103 mm, i.e. in the other stability region that is more sensitive to misalignment, and found significant instability of beam profile and signal wavelength especially in the range 1.5 - 1.6 μm. Fig. 2 shows the misalignment sensitivity of both stability regions calculated as the reciprocal of the C element of the one-way ABCD matrix [16]. The long-term stability of the signal output power and wavelength measured in the LMS

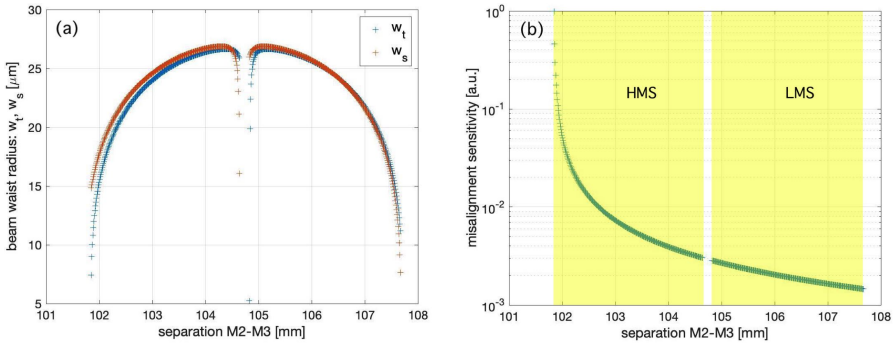

Figure 2: a) Stability regions of the astigmatically-compensated cavity (sagittal and tangential planes). b) High- and low-misalignment-sensitivity stability regions (HMS and LMS).

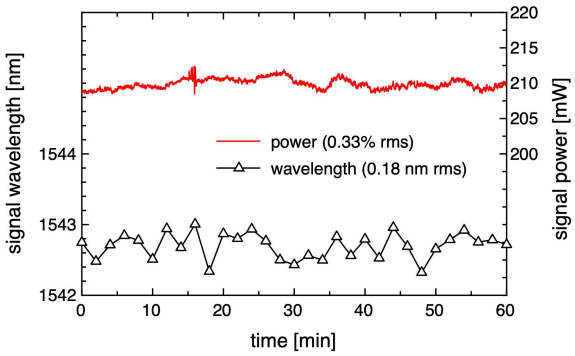

Figure 3: Output power and signal wavelength stability, with the piezo control-loop on.

region is shown in Fig. 3. Such performance, with rms fluctuation of the signal power as low as 0.33% (see Fig. 3), requires a temperature stability within ± 0.1 °C. In practice, typical room temperature control within 0.4 °C keeps power drift $< 2\%$. In the everyday use of the MgO:PPLN SPOPO with 3D printed parts, the output power and output wavelength proved to be as stable as they were with the LBO-based SPOPO.

Since the folding (incidence) angle of the curved mirrors could not be reduced to $\leq 2°$, due to constraints posed by the available mounts (an X-shaped resonator layout would have been more practical if building the SPOPO from scratch), a 2-mm BK7 Brewster-tilted plate was inserted to leave M2 and M3 at 5° incidence angle for perfect astigmatism compensation. Incidentally, as a welcome side effect, the glass plate also introduced

negative group-velocity dispersion (GVD) in the range 1.3 - 1.6 μm, where MgO:PPLN has otherwise large positive dispersion, reducing the GVD to +20 fs^2 at 1.58 μm, starting from +170 fs^2 at $\sim$ 1.3 μm where BK7 has zero dispersion.

As a consequence, the SF10 prism pair that was already set up at 180-mm separation (tip-to-tip) was actually required only for operation at the shorter wavelengths $\sim$ 1.3 μm.

The SPOPO signal wavelength could be tuned in the range 1.28 - 1.58 μm, with the exception of the water-absorption window 1.35 - 1.44 μm. No nitrogen purging was used during the SPOPO characterization, even though the system was enclosed in a box to offer this option. Another mirror set should be chosen for signal operation in the range 0.96 - 1.3 μm, allowing longer idler wavelengths up to $\sim$ 5 μm (a new MgO:PPLN crystal with proper coatings would also be necessary, as well as an IR-transmitting substrate for M2).

Although our MgO:PPLN crystal was designed for easy SPOPO tuning through translation along the fan-shaped grating (vertical) direction, we determined that our final setup must not require cover opening to access the MgO:PPLN micrometer stage, since other effective tuning means are available.

In particular, we found that once the servo-loop has been switched on for wavelength stabilization in the 1.45 - 1.58 μm range, smooth accurate tuning can be easily performed by changing the piezo setpoint. In fact, cavity length tuning of a SPOPO occurs through dispersion [5] and is more effective where the GVD is smaller (thanks to the BK7 plate). Synchronism between pump and resonant signal pulses requires that changes in signal frequency ω (or wavelength) and in cavity length L are related through the total GVD of the cavity:

$$\frac{\partial^2 \phi}{\partial \omega^2} \Delta\omega + 2\frac{\Delta L}{c} = 0 \tag{1}$$

We have calculated the signal wavelength change $\Delta\lambda_s$ for $\Delta L = 1$ μm, for all the wavelengths satisfying the phase-matching condition $|\Delta kl| < 2.78$ rad (corresponding to $sinc^2(\Delta kl/2) > 0.5$) with no additional dispersion (no prisms), being the MgO:PPLN grating at a fixed convenient $\Lambda = 21.2$ μm. The result is shown in Fig. 4a and explains why tuning is easily done with a piezo-driven actuator at 1.5 μm, where $\partial\lambda_s/\partial L$ is larger. This also explains why the open-loop SPOPO was more unstable in the HMS region, in such a spectral range. Actually, even in closed-loop condition, too close

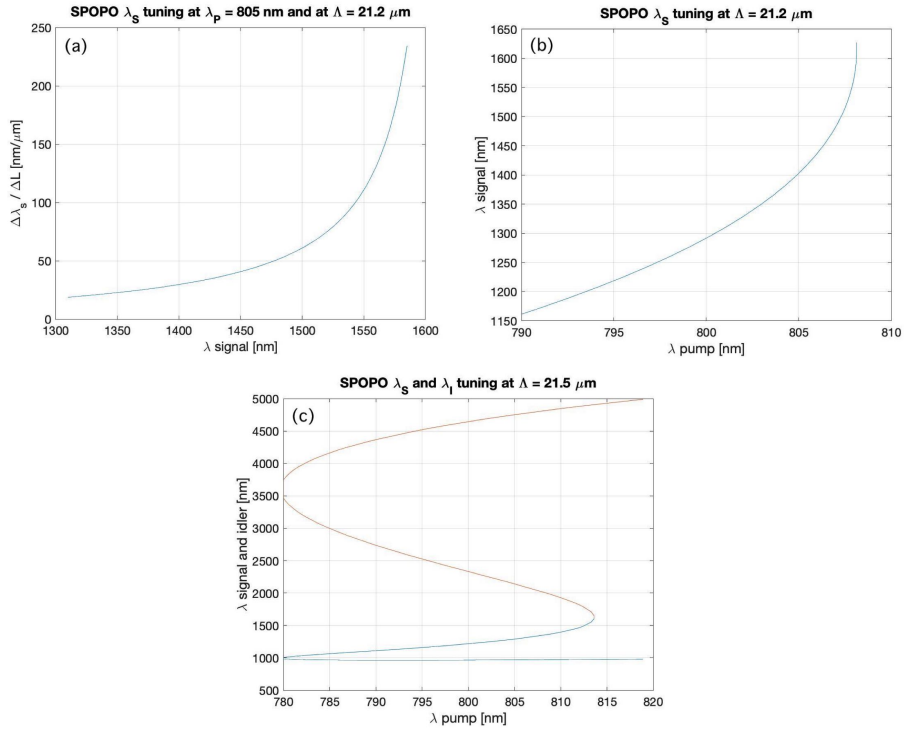

Figure 4: Tuning of signal wavelength at a convenient grating period $\Lambda = 21.2$ μm, by means of: a) cavity length changes (exact phase-matching at $\lambda_s = 1390$ nm); b) pump wavelength tuning. c) Full signal and idler range (extended to ~ 5 μm) available through moderate pump tuning around 800 nm for $\Lambda = 21.5$ μm.

to degeneracy brings such SPOPO sensitivity beyond the control range of the piezo, and the system becomes unstable [17].

The piezo was not as effective in covering the tuning range at ~ 1.3 μm: in this case it was more convenient to tune the wavelength of the pump laser. The calculated λ_s as a function of the pump wavelength λ_p, this time corresponding to ideal phase-matching $\Delta k = 0$, is shown in Fig. 4b. This same tuning method works for the whole range $\lambda_s \sim 1.3$ - 1.6 μm as well and can be considered a convenient single method for tuning this SPOPO.

Fig. 4c shows the full phase-matching curve with the typical retracing behavior, allowing to reach the mid-IR region with a mirror set suitable for $\lambda_s \sim 970$ nm.

These tuning means, either piezo/setpoint or pump wavelength, require basically a single grating spacing Λ, making the crystal choice even more affordable as a future option for mid-IR applications.

As anticipated, the SPOPO required the prism pair for generation of $\sim$ 150-fs Fourier-limited pulses in the $\sim$ 1.3 μm region, measured with a commercial non-collinear second-harmonic autocorrelator. With no prisms, the double-peak spectra suggested strongly chirped pulses and the autocorrelation traces showed pulses with significant satellites and large time-bandwidth product (TBP) [5]. However, in the $\sim$ 1.5 μm region the GVD was much smaller although still positive, and the prisms were not required to generate $\sim$ 2-times Fourier-limited $\sim$ 230-fs pulses, thanks to the negative GVD contribution of the BK7 plate. Output power and tuning performance is shown in Fig. 5. SPOPO threshold was $\sim$ 300 mW of pump power incident on the crystal. A maximum signal output power of 260 mW was obtained at 1540 nm wavelength at an incident pump power of 1.6 W at 805 nm.

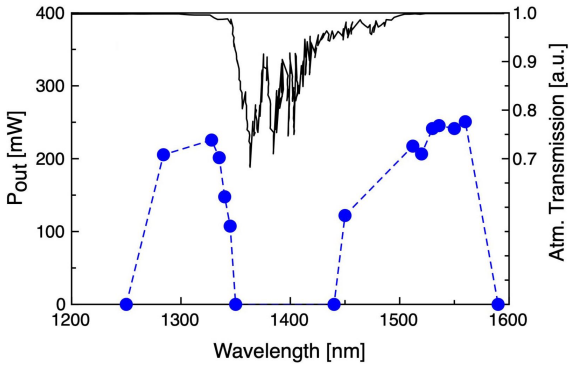

Figure 5: Tuning and output power. Total atmospheric transmission at see level in standard environmental conditions [18] is
also displayed for reference.

Pulse spectra and pulse durations are displayed in Fig. 6. Notice that prisms were inserted in the cavity only for operation at $\sim$ 1.3 μm. Their insertion loss was small compared to the OC transmittivity, hence the output power was not affected. Given the large parametric gain able to withstand significant losses, higher output power has to be expected with higher output coupling [7, 9].

3. Conclusion and future perspectives

In conclusion, we have reported the use of 3D-printed parts to realize a femtosecond SPOPO, with performance consistent with previously reported systems [5, 9]. We have found that 3D printing can be a very handy tool

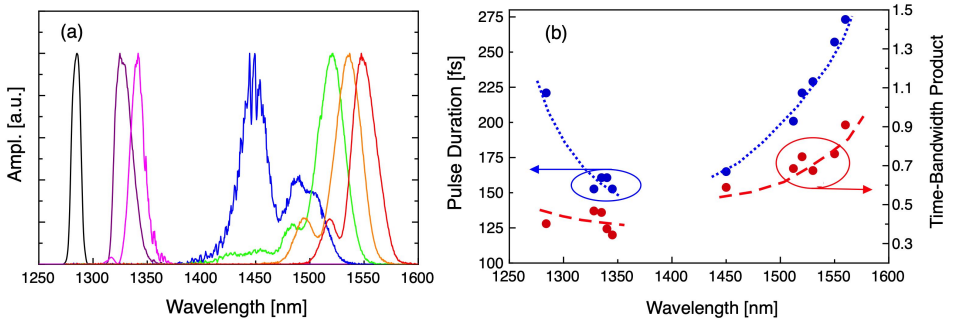

Figure 6: a) Optical spectra. b) Pulse width and TBP (0.32 is the ideal value for sech^2 pulses). Red dashed and blue dotted lines have been drawn to highlight the trend of TBP and pulse duration respectively.

for layout optimization/prototyping even for a class of relatively sensitive optical sources like femtosecond SPOPOs, before turning to professional machining for final implementation. In our case the printed PLA interfaces proved to be even suitable for long-term operation of the source, in a typical laboratory environment with temperature stability better than a fraction of 1 °C. Improved stability can be expected with lower thermal-expansion materials. More specialized high-mechanical-resistance and low-thermal-expansion 3D-printing composite or structured materials, combined with optimized low-misalignment-sensitivity optical design, might be worth to investigate in future for applications requiring particularly lightweight laser devices.

Acknowledgements. This work has been carried out in the framework of the initiative 3D@UniPV. We also wish to thank L. Tartara for useful discussions and assistance with the piezo equipment.

Declaration of Competing Interest

The Authors declare that there is no conflict of interest.

References

[1] Q. Fu, G. Mak, H. M. van Driel, "High-power, 62-fs infrared optical parametric oscillator synchronously pumped by a 76-MHz Ti:sapphire laser," Opt. Lett. 17, 1006-1008 (1992).

[2] W. S. Pelouch, P. E. Powers, C. L. Tang, "Ti:sapphire-pumped, high-repetition-rate femtosecond optical parametric oscillator," Opt. Lett. 17, 1070-1072 (1992).

[3] A. Feisst, P. Koidl, "Current induced periodic ferroelectric domain structures in LiNbO3 applied for efficient nonlinear optical frequency mixing", Appl. Phys. Letters 47, 1125-1127 (1985).

[4] L. E. Myers, R. C. Eckardt, M. M. Fejer, R. L. Byer, W. R. Bosenberg, J. W. Pierce, "Quasi-phase-matched optical parametric oscillators in bulk periodically poled LiNbO3," J. Opt. Soc. Am. B 12, 2102-2116 (1995).

[5] C. McGowan, D. T. Reid, Z. E. Penman, M. Ebrahimzadeh, W. Sibbett, D. H. Jundt, "Femtosecond optical parametric oscillator based on periodically poled lithium niobate," J. Opt. Soc. Am. B 15, 694-701 (1998).

[6] K. Devi, M. Ebrahim-Zadeh, "Room-temperature, rapidly tunable, green-pumped continuous-wave optical parametric oscillator," Opt. Lett. 42, 2635-2638 (2017).

[7] C. F. O'Donnell, S. Chaitanya Kumar, T. Paoletta, M. Ebrahim-Zadeh, "Widely tunable femtosecond soliton generation in a fiber-feedback optical parametric oscillator," Optica 7, 426-433 (2020).

[8] S. Chaitanya Kumar, B. Nandy, M. Ebrahim-Zadeh, "Performance studies of high-average-power picosecond optical parametric generation and amplification in MgO:PPLN at 80 MHz," Opt. Express 28, 39189-39202 (2020).

[9] Z. E. Penman, P. Loza-Alvarez, D. T. Reid, M. Ebrahimzadeh, W. Sibbett, D. H. Jundt, "All-solid-state mid-infrared femtosecond optical parametric oscillator based on periodically-poled lithium niobate," Opt. Commun., 146, 147-150 (1998).

[10] E. Castro-Camus, M. Koch, and A. I. Hernandez-Serrano, "Additive manufacture of photonic components for the terahertz band," J. Appl. Phys. 127, 210901 (2020).

[11] D. Rohrbach, B. J. Kang, and T. Feurer, "3D-printed THz wave- and phaseplates," Opt. Express 29, 27160-27170 (2021).

[12] B. Wijnen, P. Sanders, J. Pearce, "Improved model and experimental validation of deformation in fused filament fabrication of polylactic acid," Progress in Additive Manufacturing 3, 193-203 (2018).

[13] J. D. Kafka, M. L. Watts, J. W. Pieterse, "Synchronously pumped optical parametric oscillators with LiB3O5," J. Opt. Soc. Am. B 12, 2147-2157 (1995).

[14] J. Chesnoy, L. Fini, "Stabilization of a femtosecond dye laser synchronously pumped by a frequency-doubled mode- locked YAG laser," Opt. Lett. 11, 635-637 (1986).

[15] http://slic3r.org

[16] V. Magni, S. De Silvestri, A. Cybo-Ottone, "On the stability, mode properties, and misalignment sensitivity of femtosecond dye laser resonators," Opt. Commun. 82, 137-144 (1991).

[17] T. J. Driscoll, G. M. Gale, F. Hache, "Ti:sapphire second-harmonic-pumped visible range femtosecond optical parametric oscillator," Opt. Commun. 110, 638-644 (1994).

[18] Lord, S. D., "A new software tool for computing Earth's atmospheric transmission of near- and far-infrared radiation", nstc.rept, 1992, NASA Technical Memorandum 103957. Data collected by Gemini Observatory https://www.gemini.edu/observing/telescopes-and-sites/sites#Transmission